Marine spongin incorporation into Biosilicate® for tissue engineering applications: An in vivo study

Julia Risso Parisi[1],* , Kelly Rossetti Fernandes[2],*,
Giovanna Caroline Aparecida do Vale[2],
Alan de França Santana[2], Matheus de Almeida Cruz[2],
Carlos Alberto Fortulan[3], Edgar Dutra Zanotto[4] ,
Oscar Peitl[4], Renata Neves Granito[2] and
Ana Claudia Muniz Rennó[2]

Abstract

Biomaterials and bone grafts, with the ability of stimulating tissue growth and bone consolidation, have been emerging as very promising strategies to treat bone fractures. Despite its well-known positive effects of biosilicate (BS) on osteogenesis, its use as bone grafts in critical situations such as bone defects of high dimensions or in non-consolidated fractures may not be sufficient to stimulate tissue repair. Consequently, several approaches have been explored to improve the bioactivity of BS. A promising strategy to reach this aim is the inclusion of an organic part, such as collagen, in order to mimic bone structure. Thus, the present study investigated the biological effects of marine spongin (SPG)-enriched BS composites on the process of healing, using a critical experimental model of cranial bone defect in rats. Histopathological and immunohistochemistry analyzes were performed after two and six weeks of implantation to investigate the effects of the material on bone repair (supplemental material-graphical abstract). Histological analysis demonstrated that for both BS and BS/SPG, similar findings were observed, with signs of material degradation, the presence of granulation tissue along the defect area and newly formed bone into the area of the defect. Additionally, histomorphometry showed that the control group presented higher values for Ob.S/BS (%) and for N.Ob/T.Ar (mm^2) (six weeks post-surgery) compared to BS/SPG and higher values of N.Ob/T.Ar (mm^2) compared to BS (two weeks post-surgery). Moreover, BS showed higher values for OV/ TV (%) compared to BS/SPG (six weeks post-surgery). Also, VEGF immunohistochemistry was increased for BS (two weeks post-surgery) and for BS/SPG (six weeks) compared to CG. TGFb immunostaining was higher for BS compared to CG. The results of this study demonstrated that the BS and BS/SPG scaffolds were biocompatible and able to support bone formation in a critical bone defect in rats. Moreover, an increased VEGF immunostaining was observed in BS/SPG.

Keywords

Spongin, marine biotechnology, biomaterials, tissue engineering, biomedical application

Introduction

Bone tissue is one of the most replaced tissues of the body, with more than two million bone grafting performed annually worldwide.[1,2] In this context, biomaterials and bone grafts, with the ability of stimulating bone tissue growth and producing bone consolidation, constitute promising strategies to treat bone defects of great dimensions or non-consolidated fractures.[2,3]

In this perspective, the osteogenic effects of bioactive glasses (Bioglass 45S5) and glass-ceramics

[1]Department of Physiotherapy, Federal University of São Carlos (UFSCar), São Carlos, SP, Brazil
[2]Department of Biosciences, Federal University of São Paulo (UNIFESP), Santos, SP, Brazil
[3]Department of Mechanical Engineering, São Carlos School of Engineering São Carlos, SP, Brazil
[4]Department of Materials Engineering, Vitreous Materials Laboratory (LaMaV), Federal University of São Carlos (UFSCar), São Carlos, Brazil

*These authors contributed equally to the work.

Corresponding author:
Julia Risso Parisi, Federal University of São Carlos (UFSCar), Washington Luís, km 235, São Carlos, SP, Brazil.
Email: juliaparisi@outlook.com

(including Biosilicate®) must be highlighted.[4–11] Bioglass 45S5 (BG) and Biosilicate (BS) (Na_2O–CaO–SiO_2–P_2O_5 system) have the ability to bond to bone tissue, forming an apatite layer on their surface, which acts as a template for newly bone formation.[10,12,13] Especially BS, a fully crystallized glassceramic, has been demonstrating stimulatory effects on bone metabolism and on the process of fractures healing.[4–6,9–12,14] Despite its well-known positive effects of BS on osteogenesis, its use as bone grafts in critical situations such as bone defects of high dimensions or in non-consolidated fractures (in osteoporotic patients for example) may not be sufficient to stimulate tissue healing.[15,16]

Consequently, several approaches have been explored to improve the bioactivity of BS.[11,15] A promising strategy to optimize the biological effects of BS is the introduction of an organic part, such as collagen (Col) in order to mimic bone structure.[15–17]

It is known that Col is the most abundant protein of body and the major component of the extracellular matrix (ECM).[18] It is biocompatible, has a high affinity to water, controllable biodegradation, hemostatic properties, low inflammatory host response, being a very useful material to be used in biomedical applications.[14,19]

The most common sources of Col are from bovine and porcine origin; however, they have been a matter of concern mainly due to religious constraints related with avoidance of porcine and bovine products, to the recent episodes of the wide scale bovine spongiform encephalopathy (BSE) outbreak in bovines and also to the high manufacturing and production costs.[14,19] For these reasons, different sources of Col to be used in the tissue engineering field have been explored such as the ones from marine sponges.[20–22] Marine sponge Col or spongin (SPG) (which is similar to Type XIII Col), is an excellent alternative for Col extraction, with a low risk of transmission of infection-causing agents and good biocompatibility.[19,20] Also, it has been demonstrated that SPG is able of accelerating osteoblast cell proliferation in in vitro studies, showing an osteogenic potential.[23–25]

In view of the growing demand for developing composites with improved osteogenic properties to be used as off-the-shelf available bone substitutes and based on the singularity of the marine biodiversity for providing resources of bioactive compounds, it was hypothesized that the addition of SPG might improve the biological performance of BS. Thus, the aim of the current in vivo study is to evaluate the orthotopic in vivo response to BS/SPG composites in rats. Pre-set scaffolds in different formulations were implanted in a cranial bone defects in rats. Histocompatibility (orthotopic implants; histology, histomorphometry and immuhistochemistry) was evaluated after 15 and 45 days post-surgery.

Materials and methods

Biomaterials

SPG was extracted from the marine sponge *Aplysina fulva* (collected in Praia Grande 23o49'23.76 "S, 45o25'01.79" W, São Sebastião, Brazil) based on the method described by Swatschek et al..[26] Samples were collected and stored in sea water until to be submitted to the procedures of extraction. For this, samples were washed three times in Milli-Q water for debris removal and were immediately stored at $-20°C$. Species were then cut into small pieces and placed in Tris-HCl buffer (100 mM, pH 9.5, 10 mM EDTA, 8 M urea, 100 mM 2-mercaptoethanol). NaOH solution was added to adjust the pH to 9. Solution was transferred into a stirred beaker during 24 h and centrifuged for 5 min, at $2°C$. The pellet was discarded, and the supernatant was removed. Afterwards, the pH was adjusted again to 4 using acetic acid solution and a precipitate was obtained. This precipitate was resuspended in Milli-Q water, centrifuged one more time and lyophilized for preservation.[26]

For this study, BS (particle size 250–1000 μm) which is a fully crystallized bioactive ceramic of the quaternary P_2O_5–Na_2O–CaO–SiO_2 system/patent application WO2004/074199) was used (Vitreous Materials Engineering, Federal University of São Carlos, São Carlos, SP, Brazil). Additionally, carboxymethyl cellulose (CMC), density 1.59 g/cm^3, was provided by Sigma Aldrich (Missouri, USA). Poly (methyl methacrylate) (PMMA, particle size: 15 μm) and methyl methacrylate (MMA, purity: 99.09%) was provided by VIPI Produtos Odontológicos (Pirassununga, São Paulo, Brazil) (the polymers were used with the purpose of aggregating BS and SPG).

Scaffold preparation

Scaffolds, with two different formulations, were used in this study: BS 100% and BS (80%) and SPG (20%). PMMA was used to aggregate the materials. In addition, CMC was used to produce pores into the samples (around 60%).[27–29] For manufacturing, materials were weighted (Table 1), put in a silicone container with distilled water and mixed. After that, MMA monomer was added, mixed again and transferred to a silicon mold (8 mm × 2 mm). Subsequently, the molds were sealed, submitted to a pressure air chamber (at 0.6 MPa) for 30 min and vacuum dried (10^{-3} Torr) for 15 min. Samples were then, removed from the silicon

Table 1. Experimental formulations of composites expressed in grams (g).

Groups	PMMA (g)	MMA (g)	BS (g)	SPG (g)	CMC (g)	Water (g)
BS	0.236	0.472	0.560	0	0.043	0.565
BS/SPG	0.236	0.472	0.368	0.092	0.043	0.565

molds, packaged and sterilized by ethylene oxide (Acecil, Campinas, SP, Brazil).

In vivo studies

Male Wistar rats (12 weeks, weight 300–350 g) were randomly distributed into three groups ($n = 12$) (control group: CG; BS: Biosilicate and BS/SPG 80/20: Biosilicate and spongin). Animals were distributed into two sub-groups with different times of euthanasia (15 and 45 days). The animals were maintained under controlled temperature ($22 \pm 2°C$), light–dark periods of 12 h and had free access to water and standard food. This study was approved by the Animal Care Committee guidelines of the Federal University of São Paulo (CEUA n° 6544170217).

For the surgical procedures, rats were submitted to anaesthesia with a combination of ketamine (80 mg/kg), xylazine (8 mg/kg), acepromazine (1 mg/kg) and fentanyl (0.05 mg/kg). Animals were immobilized and had their skulls shaved, washed and disinfected with povidone-iodine. Using aseptic techniques, an incision was made through the skin and the periosteum was removed, for bone exposure. A 8 mm defect was created in the parietal region using a trephine drill (3i Implant Innovations Inc., Palm Beach Gardens, USA) under copious saline irrigation.[30,31] The implants were placed in the created defect, according to a randomization scheme. The wound was closed with resorbable Vicryl® 5–0 (Johnson & Johnson, St. Stevens-Woluwe, Belgium) after which the skin was also sutured with nylon (Agraven®; InstruVet BV, Cuijk, The Netherlands). Four animals were housed per cage and the intake of water and food was monitored in the initial post-operative period. Further, rats were given appropriate postoperative care and animals were observed for signs of pain, infection and proper activity. After the experimental periods, animals were euthanized by CO_2 for sample removal.

Histological procedures

Skulls were fixated in 4% formaldehyde for 24 h, followed by dehydration in a graded series of ethanol and embedding in methylmethacrylate (MMA). After polymerization of the specimens, histological analysis was done. Therefore, thin sections (5 μm) were obtained (in a perpendicular direction, to the medial-lateral drilling axis of the implants) using a microtome with a tungsten carbide disposable blade (Leica TC65, Leica Microsystems SP 1600, Nussloch, Germany). Samples were stained with Goldner Trichrome.

At least three sections of each specimen were examined using light microscopy (Leica Microsystems AG, Wetzlar, Germany). A qualitative analysis was performed considering the following parameters: presence of granulation tissue, newly formed bone, osteoid and biomaterial particles. The analysis was performed in a blinded way by two experienced researchers (G.C.A.V and J.R.P.). Also, illustrative photomicrographies representing an overview of the bone defect area were performed using the software OsteoMeasure System (Osteometrics, Atlanta, GA, USA) for all groups.[5]

Histomorphometric analysis

Samples were quantitatively scored trough OsteoMeasure System (Osteometrics, Atlanta, GA, USA). First, the region of interest (ROI) was defined as all the region of the defect, from its right border through the left. The mean tissue area (T.Ar) analyzed was 3.01 ± 1.41 mm^2. For that, the following parameters were evaluated: bone volume as a percentage of tissue volume (BV/TV, %), osteoid volume as a percentage of tissue volume (OV/TV, %), osteoid thickness (O.Th, μm), osteoblastic surface as a percentage of the bone surface (Ob.S/BS, %) and number of osteoblasts per unit of tissue area (N.Ob/T.Ar,/mm^2). In addition, the analysis was performed by one experienced observer (G.C.A.V.) in a blinded way.

Immunohistochemistry analysis

For immunohistochemistry analysis, the protocol which was described previously was used,[32] using the streptavidin-biotin-peroxidase method. Resin from the sections was removed with xylene/chloroform (1:1), rehydrated in graded ethanol and pretreated with 0.01 M citric acid buffer (pH 6) in a steamer for 5 min. The endogenous peroxidase was inactivated using hydrogen peroxide in phosphate-buffered saline (PBS) for 5 min and blocked with 5% normal goat serum in PBS for 10 min. The primary antibody was incubated with anti-vascular endothelial growth factor (anti-VEGF, Santa Cruz Biotechnology, USA) at a concentration of 1:200 and anti-transforming growth factor beta (anti-TGF-b, Santa Cruz Biotechnology, USA) also at a concentration of 1:200 for 2 h. Then,

biotin-conjugated secondary antibody was incubated with anti-rabbit IgG (Vector Laboratories, Burlingame, CA, USA) at a concentration of 1:200 in PBS was used (for 30 min). Samples were incubated with avidin biotin complex conjugated to peroxidase for 30 min. A solution of 3–3′-diaminobenzidine solution was used to reveal the immunostaining (5 min) and restained with Harris haematoxylin (Merck) for 4 min. A light microscopy (Leica Microsystems AG, Wetzlar, Germany) were used for qualitative analysis (presence and location of the immunomarkers) and semiquantitative evaluation according to a previously described scoring scale from 1 to 4: 1 = absent (0% of immunostaining), 2 = weak (1–35% of immunostaining), 3 = moderate (36–67% of immunostaining), and 4 = intense (68–100% of immunostaining).[32] The analysis was performed in a blinded way by three experienced researchers (G.C.A.V., J.R.P. and K.R.F.).

Statistical analysis

Data were analysed and displayed in graphs, and the values were expressed as mean and standard deviation. In the statistical analysis, the distribution of variables was tested using the Shapiro–Wilk normality test. For the analysis of multiple comparisons, ANOVA was used with post hoc Tukey for parametric data and nonparametric data, and the Kruskal–Wallis test was used with post hoc Dunn. The level of significance was set at 5% ($p \leq 0.05$). All statistical analyses were performed using GraphPad Prism version 6.01.

Results

Histological analysis

An illustrative overview of the defect area of all experimental groups, two and six weeks post-surgery, is shown in Figure 1. For CG, two weeks post-surgery, newly formed bone was observed throughout the defect, with some areas of osteoid. For BS and BS/SPG, bone defect area was filled mainly by biomaterial particles, with some spare areas of newly formed bone and osteoid. Six weeks post-surgery, thickness area of the bone defect for CG decreased and a larger amount of bone could be seen. For BS-treated animals, the thickness of the bone defect seems to be lower, with some degradation of the biomaterial, surrounded by osteoids and areas of newly formed bone. For BS/SPG, the thickness of bone defect remained similar to the other experimental period, with the presence of some osteoids and newly formed bone.

Figure 2 shows the photomicrographs of the qualitative histological analysis of all experimental groups (two and six weeks post-surgery).

Two weeks post-surgery, no sign of inflammatory process was observed for any group. CG presented some areas of the newly formed bone, especially at the edges and center of the defect, with the presence of osteoids and granulation tissue (Figure 2(a)). For BS, most of the defect was filled by granulation tissue, with newly formed bone observed at the edges (Figure 2(b)). Also, initial degradation of the implanted biomaterial was verified. For BS/SPG, granulation tissue was presented in most of the defect area, with some osteoids and newly formed bone. Additionally, for most of the samples, particles of the biomaterial were presented in the defect region (Figure 2(c)).

After six weeks post-surgery, CG presented areas of woven bone with a more mature aspect and newly formed bone in all extension of the defect (Figure 2(d)). In addition, granulation tissue and osteoids could be observed in all extension of the defect. For BS, degradation of the material was verified in the defect area but some particles still could be seen, surrounded by granulation tissue and some newly formed bone (Figure 2(e)). For BS/SPG, an intense degradation of the material was observed, with the presence of few remaining particles, surrounded by portions of osteoids (Figure 2(f)). Furthermore, for these animals, it was possible to observe the presence of newly formed bone in all extension of the defect and with a mature aspect in the margin (Figure 2(f)).

Histomorphometric analysis

The histomorphometric analysis demonstrated that no statistical difference was observed for BV/TV (%) among groups, two and six weeks post-surgery (Figure 3).

Figure 4(a) demonstrated a higher mean value of OV/TV (%) for CG when compared to BS ($p = 0.0089$) after two weeks. In addition, six weeks post-surgery, BS showed higher values for this variable compared to BS/SPG ($p = 0.0387$). Also, for O.th (μm), no statistical difference was found among groups for both the experimental periods (Figure 4(b)).

For Ob.S/BS (%) (Figure 5(a)), no statistical difference was found among groups after two weeks post-surgery. However, CG presented higher values for this variable compared to BS/SPG ($p = 0.045$). Also, for N.Ob/T.Ar (mm²), a significant higher values ($p = 0.0284$) was found for CG compared to BS after two weeks. Six weeks post-surgery, a higher value ($p = 0.0024$) was verified for CG compared to BS/SPG (Figure 5(b)).

Immunohistochemistry analysis

VEGF immunostaining. Figure 6 represents the qualitative immunohistochemistry analysis of VEGF for CG, BS

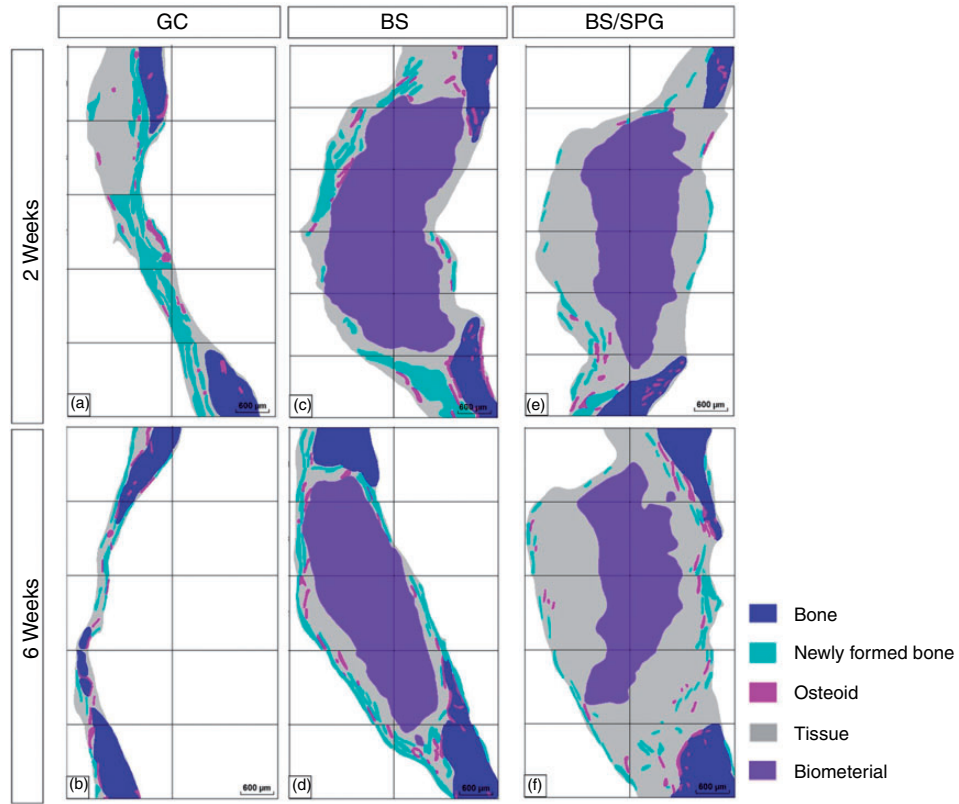**Figure 1.** Overview of all the experimental groups: Control (a, b); BS (c, d); BS/SPG (e, f) after two and six weeks post-surgery. Scale bar $= 600\,\mu$m.
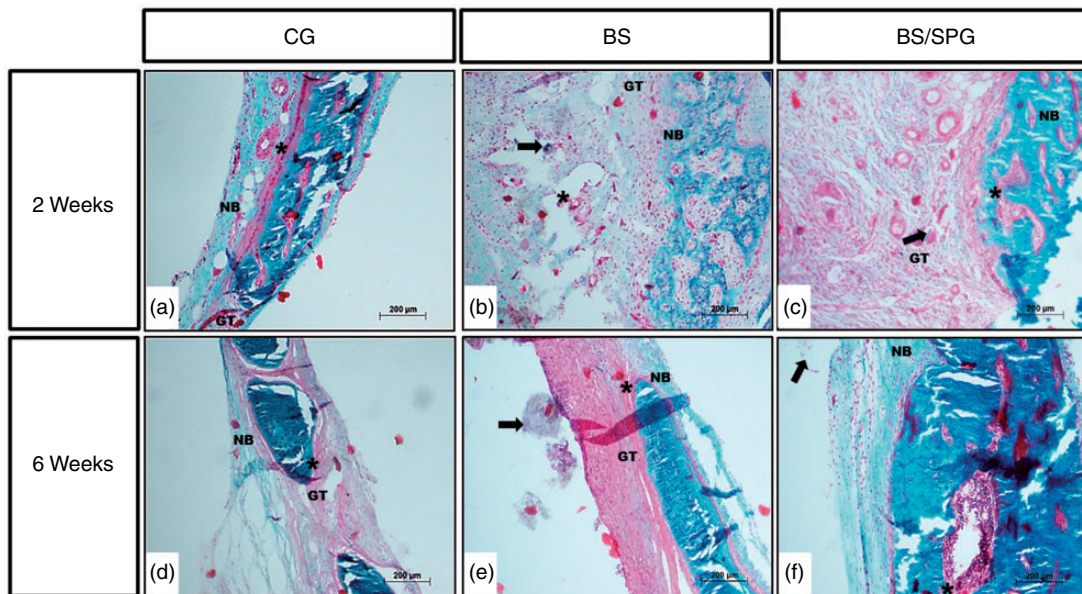

Figure 2. Representative histological sections of cranial bone defects of the groups: Control (a, d); BS (b, e); BS/SPG (c, f) after two and six weeks, respectively. Newly formed bone (NB), granulation tissue (GT), osteoid (*), residual material (black arrow). Bar represents $200\,\mu$m. (mag. $\times10$). Goldner Trichrome stain.

and BS/SPG groups two and six weeks post-surgery. For both periods, VEGF immunostaining was observed in the connective tissue fibers along the bone defect in CG (Figure 6(a) and (d)). For BS and BS/SPG, VEGF immunostaining was verified around the particles of the materials and in the connective

tissue throughout the bone defect after two and six weeks (Figure 6(b), (c), (e) and (f)). Furthermore, for BS/SPG in both periods, VEGF immunostaining was also observed in the granulation tissue (Figure 6 (c) and (f)).

Figure 7 demonstrated the semi-quantitative analysis of VEGF immunostaining after two and six weeks post-surgery. In the first period analyzed, a higher value of VEGF immunostaining was observed in the BS compared to CG ($p = 0.0182$). Additionally, BS/SPG demonstrated a higher value of VEGF immunostaining compared to CG ($p = 0.0256$) after six weeks post-surgery.

TGF-b immunostaining. Figure 8 represents the qualitative immunohistochemical analysis of TGF-b for CG, BS and BS/SPG two and six weeks post-surgery. For CG in both periods (Figure 8[a] and 8[d]) it is possible to observe that TGF-b immunolabeling predominantly immunostaining in the connective tissue fibers present along bone defect. For BS and BS/SPG, TGF-b immunostaining was verified around the particles of the materials and in the connective and granulation tissue
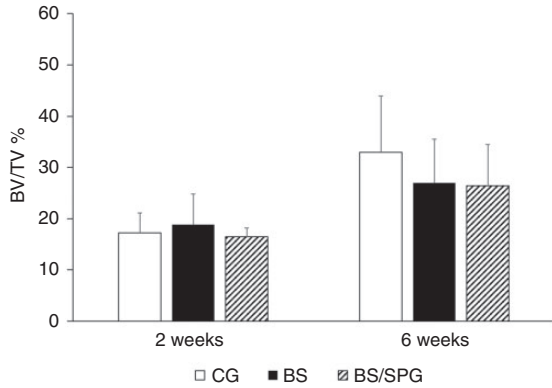

Figure 3. Means and standard deviation of BV/TV for the CG, BS and BS/SPG after two and six weeks post-surgery. Dunn's test.
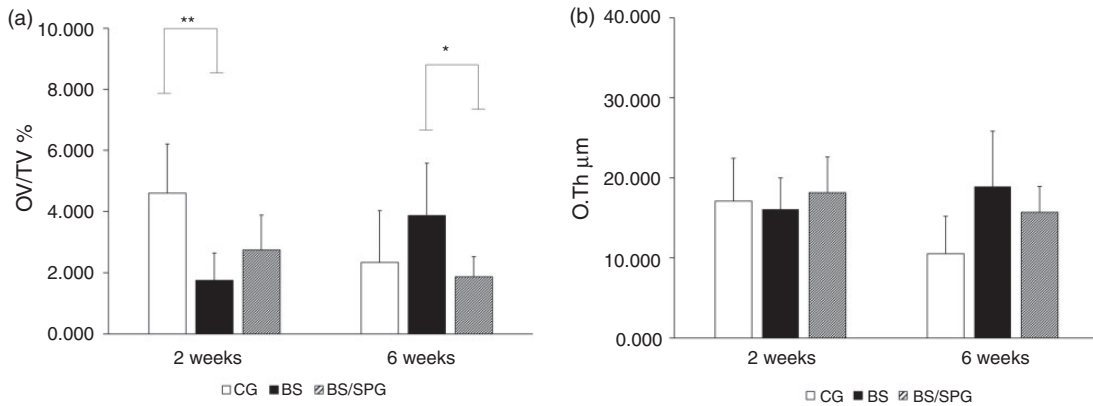

Figure 4. Figure 4. Means and standard deviation of OV/TV (a); and O.Th (b) for the CG, BS and BS/SPG after two and six weeks post-surgery. Dunn's test. *p<0.05 and **p<0.01.
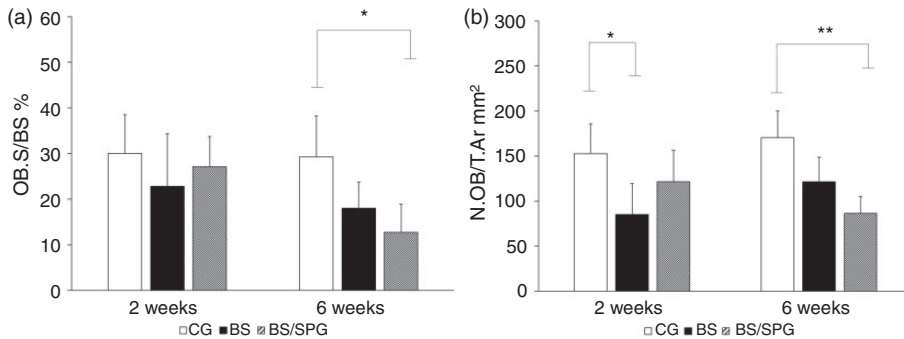

Figure 5. Means and standard deviation of OB.S/BS (a); and N.OB/T.Ar (b) for the CG, BS and BS/SPG after two and six weeks post-surgery. Dunn's test. *p<0.05 and **p<0.01.
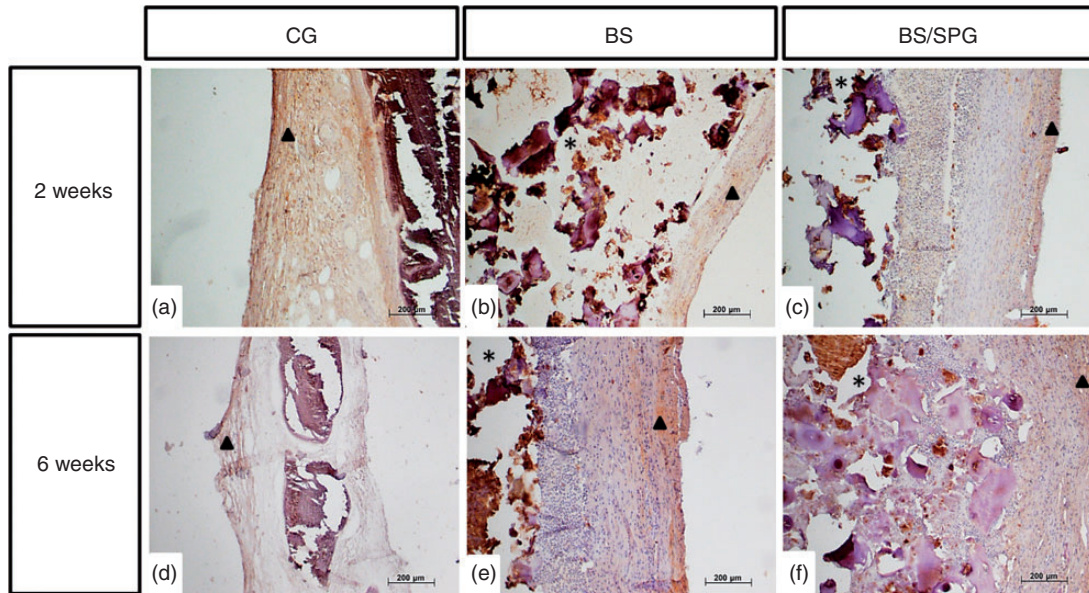
Figure 6. Representative histological sections of VEGF immunohistochemistry for CG (a and d), BS (b and e) and BS/SPG(c and f), two and sixweeks postsurgery. Biomaterial (*) and VEGF immunostaining (▲). Scale bar: 200 mm (mag. 10).
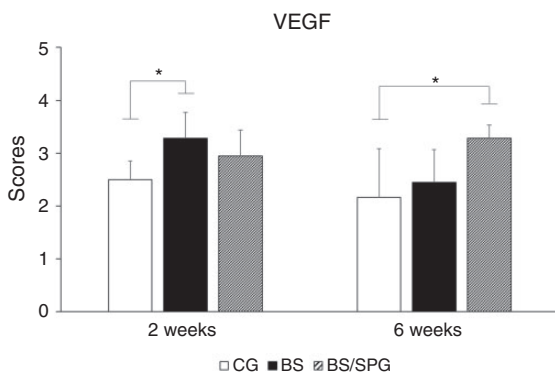

Figure 7. Means and SD scores of immunohistochemistry of VEGF after two and six weeks. *$p < 0.05$.

throughout the bone defect (two and six weeks post-surgery) (Figure 8(b), (c), (e) and (f)).

Figure 9 presents the semi-quantitative analysis of TGF-β immunostainig two and six weeks post-surgery. No significant difference was observed among the others groups analyzed in the first period. Furthermore, after six weeks, a higher value was observed for TGF-β immunostaining in the BS compared to CG ($p = 0.049$).

Discussion

The present study investigated the biological effects of SPG-enriched BS composites on the process of healing, using a critical experimental model of cranial bone defect in rats. Histological analysis demonstrated that for both BS and BS/SPG, similar findings were

observed, with signs of material degradation, the presence of granulation tissue along the defect area and newly formed bone. Interestingly, for these groups, the thickness of the defect was higher compared to CG. Histomorphometry showed no difference for BV/TV among groups. Furthermore, CG presented higher values for Ob.S/BS (%) and for N.Ob/T.Ar (mm^2) (six weeks post-surgery) compared to BS/SPG and higher values of N.Ob/T.Ar (mm^2) compared to BS (two weeks post-surgery). Moreover, BS showed higher values for OV/TV (%) compared to BS/SPG (six weeks post-surgery). Also, VEGF immunolabelling was increased for BS (two weeks post-surgery) and for BS/SPG (six weeks) compared to CG. TGFb immunostaining was higher for BS compared to CG.

Many authors demonstrated the stimulatory effects of BS on bone tissue metabolism.[5,8,9,11] Histological findings demonstrated that BS scaffolds (with or without Col) degraded over time, liberating space into the defect area and allowing tissue ingrowth. Also, it is important to emphasize that no inflammatory response was observed in the biomaterial-treated animals, indicating the biocompatibility of BS and SPG. It is well known that ionic dissolution products of BS have been shown to beneficially affect osteogenesis by the formation of a silica-rich layer which acts as a template for calcium phosphate precipitation and directs new bone formation.[12,16,33,34] Furthermore, combining materials with the aim of obtaining bone biomimetic composites (for example, BS and Col) may be a very promising strategy for bone tissue engineering proposals. Composites mimicking bone composition such as the
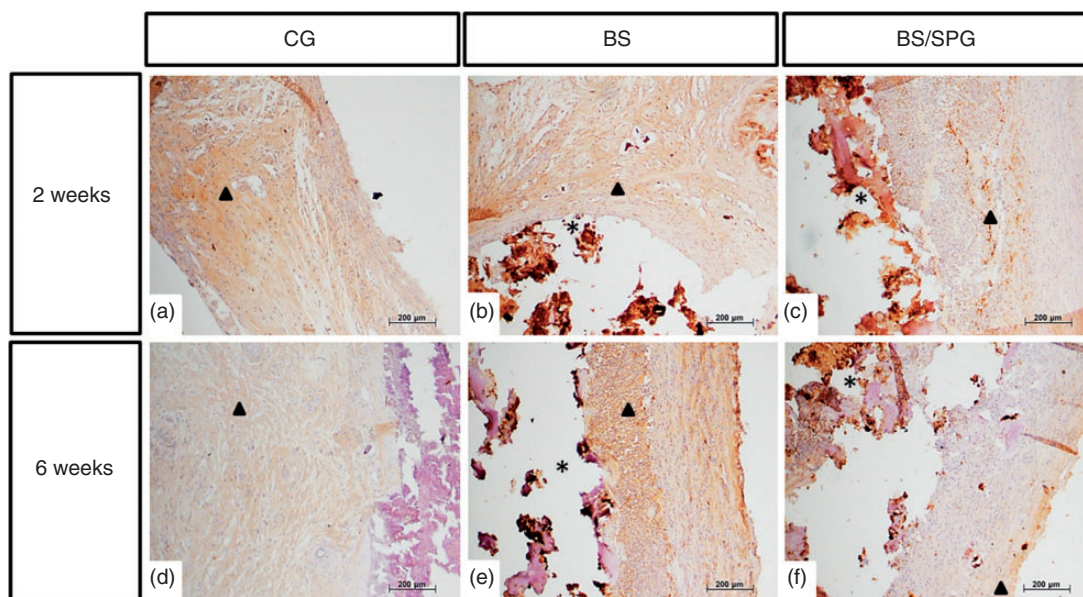
Figure 8. Representative histological sections of transform growth factor beta (TGF-b) immunohistochemistry of the CG (a and d), BS (b and e) and BS/SPG (c and f) experimental groups, after two and six weeks post-surgery. TGF-b immunostaining (▲) and biomaterial (*). Scale bar: 200 mm (mag. 10).
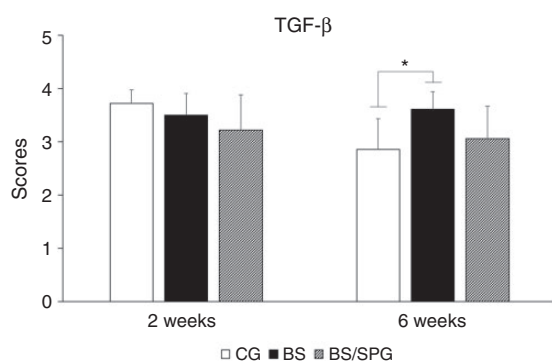

Figure 9. Means and SD scores of immunohistochemistry of TGF-β after two and six weeks. *$p < 0.05$.

association of Col (representing the organic part) with BG (the inorganic part) have been demonstrating improved biological properties in the process of bone healing.[24,35,36] However, in the present study, the addition of SPG (at the percentage of 20%) was not able to produce increased bone tissue deposition. Two hypotheses for this finding could be raised: (i) the amount of SPG was not sufficient to improve the stimulatory effect of BS; (ii) the rate of bioactivity of BS was high enough to stimulate the bone tissue growth, preventing an extra effect of SPG.

Moreover, histomorphometric findings showed that, besides the similar amount of mineralized bone inside the defect, the presence of osteoid tissue was higher in BS than in BS/SPG at six weeks. Interestingly, at the same time point, only BS/SPG exhibited a lower

number of osteoblasts and lower osteoblastic surface than CG. It is well known that, as BS degrades, the ionic products of its dissolution are able to stimulate the osteoblast recruitment, growth, osteogenic differentiation and matrix deposition.[29,36] So, even if any cells are required for the growth of bone mineral on the surface of a bioactive glass at the beginning of the process, cell activity and function may also be enhanced by the local chemical environment created by BS.[37] Therefore, another hypothesis could be raised: the presence of SPG in a composite slows the ionic release by the bioactive material, making the healing process more gradual, which could be particularly favorable for clinical applications in which the rate of the natural tissue ingrowth into the material is also expected to be slower (for instance in the case of vascular impairment), avoiding the total material resorption before complete tissue regeneration.

Also, the process of tissue repair and bone consolidation is highly dependent of an adequate vascularization and blood perfusion at the area of the injury.[38,39] In the present study, higher VEGF immunolabelling was observed for BS (two weeks post-implantation) and BS/SPG (six weeks post-implantation). It has been reported that BS has a stimulatory effect on neovascularization by stimulating the secretion of angiogenic factors,[10,17] which together with the osteopromotive properties of BS might further influence bone formation. Furthermore, Liu et al.,[3] using a biomimetic material (containing collagen), observed a positive immunostaining for VEGF factor in a defect

of rat calvaria. The authors observed that the biomimetic materials that showed greater VEGF immunostaining exhibited superior regeneration properties characterized by the profuse deposition of new bone structures and vascularization in the middle of defect.

Furthermore, the immunohistochemistry analysis demonstrated an increased immunolabeling of TGFb in the BS, 15 days post-surgery. It is well known that the TGFb plays a critical role in bone remodeling, stimulating matrix protein synthesis and bone cell proliferation.[40] In this context, the higher immunolabelling observed for BS may have influenced the activity and proliferation of osteoblast cells, which may be related to the increased newly formed bone deposition. TGFb is known to induce osteogenic differentiation of BMSCs and enhance calvarial defect healing.[40] Carinci et al.[41] demonstrated an increase inTGFb expression in an in vitro study in cells cultivated in the presence of PerioGlass (a material with similar properties of BS). Interestingly, the enrichment of glass ceramic with SPG did not affect the TGFb expression.

Based on the above considerations, the introduction of SPG into BS was effective in increasing VEGF immunolabeling, which may have increased the blood supply. However, the biological performance of the scaffolds was not optimized by this strategy evidenced by the similar results of the histological analysis. Possibly, this lack of results is related to the percentage of SPG added to BS which was not sufficient to produce an extra effect. However, based on the stimulatory effects of BS and SPG on tissue healing, further studies are needed to investigate the effects of this composite, especially using a higher concentration of SPG.

Conclusions

In summary, this study demonstrated that the BS and BS/SPG scaffolds were biocompatible and able to support bone formation in a critical bone defect in rats. Moreover, BS/SPG modulated the immunoexpression of VEGF.

Declaration of conflicting interests

The author(s) declared no potential conflicts of interest with respect to the research, authorship, and/or publication of this article.

ORCID iDs

Julia Risso Parisi (ID) https://orcid.org/0000-0002-4325-0638
Edgar Dutra Zanotto (ID) https://orcid.org/0000-0003-4931-4505

Supplemental material

Supplemental material for this article is available online.

References

1. Campana V, Milano G, Pagano E, et al. Bone substitutes in orthopaedic surgery: from basic science to clinical practice. *J Mater Sci Mater Med* 2014; 25: 2445–2461.
2. Wangao W and Yeung KWK. Bone grafts and biomaterials substitutes for bone defect repair: a review. *Bioact Mater* 2017; 2: 224–247.
3. Liu M, Nakasaki M, Shih YV, et al. Effect of age on biomaterial-mediated in situ bone tissue regeneration. *Acta Biomater* 2018; 78: 329340.
4. Bossini PS, Renno AC, Ribeiro DA, et al. Biosilicate® low-level laser therapy improve bone repair in osteoporotic rats. *J Tissue Eng Regen Med* 2011; 5: 229–237.
5. Fernandes KR, Magri AMP, Kido HW, et al. Characterization and biological evaluation of the introduction of PLGA into biosilicate((R)). *J Biomed Mater Res Part B Appl Biomater* 2017; 105: 1063–1074.
6. Granito RN, Ribeiro DA, Renno AC, et al. Effects of biosilicate and bioglass 45S5 on tibial bone consolidation on rats: a biomechanical and a histological study. *J Mater Sci Mater Med* 2009; 20: 2521–2526.
7. Kido HW, Oliveira P, Parizotto NA, Crovace MC, et al. Histopathological, cytotoxicity and genotoxicity evaluation of Biosilicate(R) glass-ceramic scaffolds. *J Biomed Mater Res A* 2013; 101: 667–673.
8. Kido HW, Brassolatti P, Tim CR, et al. Porous poly (D, L-lactide-co-glycolide) acid/biosilicate(R) composite scaffolds for bone tissue engineering. *J Biomed Mater Res Part B Appl Biomater* 2015; 105: 63–71.
9. Matsumoto MA, Caviquioli G, Biguetti CC, et al. A novel bioactive vitroceramic presents similar biological responses as autogenous bone grafts. *J Mater Sci Mater Med* 2012; 23: 1447–1456.
10. Moura J, Teixeira LN, Ravagnani C, et al. In vitro osteogenesis on a highly bioactive glass-ceramic (Biosilicate). *J Biomed Mater Res A* 2007; 82: 545–557.
11. Renno AC, Bossini PS, Crovace MC, et al. Characterization and in vivo biological performance of biosilicate. *Biomed Res Int* 2013; 2013: 1–7.

12. Hench LL, Xynos ID and Polak JM. Bioactive glasses for in situ tissue regeneration. *J Biomater Sci Polym* 2004; 15: 543–562.

13. Välimäki VV and Aro HT. Molecular basis for the action of bioactive glasses as bone graft. *Scand J Surg* 2006; 95: 95–102.

14. Rizwan M, Hamdi M and Basirun WJ. Bioglass(R) 45S5-based composites for bone tissue engineering and functional applications. *J Biomed Mater Res A* 2017; 105: 3197–3223.

15. Nijsure MP, Pastakia M, Spano J, et al. Bioglass incorporation improves mechanical properties and enhances cell-mediated mineralization on electrochemically aligned collagen threads. *J Biomed Mater Res A* 2017; 105: 2429–2440.

16. Crovace MC, Souza MT, Chinaglia CR, et al. Biosilicate® – a multipurpose, highly bioactive glass-ceramic: In vitro, in vivo and clinical trials. *J Non Crystall Solids* 2015; 432: 90–110.

17. Marelli B, Ghezzi CE, Barralet JE, et al. Three-dimensional mineralization of dense nanofibrillar collagen-bioglass hybrid scaffolds. *Biomacromolecules* 2010; 11: 1470–1479.

18. Girlanda FF, Feng HS, Corrêa MG, et al. Deproteinized bovine bone derived with collagen improves soft and bone tissue outcomes in flapless immediate implant approach and immediate provisionalization: a randomized clinical trial. *Clin Oral Invest* 2019; 23: 3885–3893.

19. Nelson C, Khan Y and Laurencin CT. Nanofiber/microsphere hybrid matrices in vivo for bone regenerative engineering: a preliminary report. *Regen Eng Transl Med* 2018; 4: 133–141.

20. Lin Z, Solomon KL, Zhang X, et al. In vitro evaluation of natural marine sponge collagen as a scaffold for bone tissue engineering. *Int J Biol Sci* 2011; 7: 968–977.

21. Silva TH, Moreira-Silva J, Marques AL, et al. Marine origin collagens and its potential applications. *Mar Drugs* 2014; 12: 5881–5901.

22. Parisi JR, Fernandes KR, Avanzi IR, et al. Incorporation of collagen from marine sponges (spongin) into hydroxyapatite samples: characterization and in vitro biological evaluation. *Mar Biotechnol* 2018; 21: 30–37.

23. Exposito JY, Cluzel C, Garrone R, et al. Evolution of collagens. *Anat Rec* 2002; 268: 302–316.

24. Green D, Howard D, Yang X, et al. Natural marine sponge fiber skeleton: a biomimetic scaffold for human osteoprogenitor cell attachment, growth, and differentiation. *Tissue Eng* 2003; 9: 1159–1166.

25. Iwatsubo T, Kishi R, Miura T, et al. Formation of hydroxyapatite skeletal materials from hydrogel matrices via artificial biomineralization. *J Phys Chem B* 2015; 119: 8793–8799.

26. Swatschek D, Schatton W, Kellermann J, et al. Marine sponge collagen: isolation, characterization and effects on the skin parameters surface-pH, moisture and sebum. *Eur J Pharm Biopharm* 2002; 53: 107–113.

27. Sousa THS, Fortulan CA, Antunes ES, et al. Concept of a bioactive implant with functional gradient structure. *KEM* 2019; 396: 221–224.

28. Lopez-Heredia MA, Sa Y, Salmon P, et al. Bulk properties and bioactivity assessment of porous polymethylmethacrylate cement loaded with calcium phosphates under simulated physiological conditions. *Acta Biomater* 2012; 8: 3120–3127.

29. Haach LCA, Purquerio BM, Silva NF, Jr, et al. Comparison of two composites developed to be used as bone replacement – PMMA/bioglass 45S5® microfiber and PMMA/hydroxyapatite. *Bioceram Develop Appl* 2014; 4: 71.

30. Luvizuto ER, Queiroz TP, Margonar R, et al. Osteoconductive properties of β-tricalcium phosphate matrix, polylactic and polyglycolic acid gel, and calcium phosphate cement in bone defects. *J Craniofac Surg* 2012; 23: e430–433.

31. Kubota T, Hasuike A, Ozawa Y, et al. Regenerative capacity of augmented bone in rat calvarial guided bone augmentation model. *J Periodontal Implant Sci* 2017; 47: 77–85.

32. Magri AMP, Fernandes KR, Assis L, et al. Photobiomodulation and bone healing in diabetic rats: evaluation of bone response using a tibial defect experimental model. *Lasers Med Sci* 2015; 30: 1949–1957.

33. Pinto KNZ, Tim CR, Crovace MC, et al. Scaffolds of bioactive glass-ceramic (Biosilicate®) and bone healing: a biological evaluation in an experimental model of tibial bone defect in rats. *Biomed Mater Eng*. 2018; 29: 665–683.

34. Granito RN, Rennó AC, Ravagnani C, et al. In vivo biological performance of a novel highly bioactive glass-ceramic (Biosilicate®): a biomechanical and histomorphometric study in rat tibial defects. *J Biomed Mater Res Part B Appl Biomater* 2011; 97: 139–147.

35. Ueno FR, Kido HW, Granito RN, et al. Calcium phosphate fibers coated with collagen: in vivo evaluation of the effects on bone repair. *Biomed Mater Eng* 2016; 27: 259–273.

36. Xynos ID, Hukkanen MV, Batten JJ, et al. Bioglass 45S5 stimulates osteoblast turnover and enhances bone formation in vitro: implications and applications for bone tissue engineering. *Calcif Tissue Int* 2000; 67: 321–329.

37. Gao C, Peng S, Feng P, et al. Bone biomaterials and interactions with stem cells. *Bone Res* 2017; 5: 17059.

38. Yang YQ, Tan YY, Wong R, et al. The role of vascular endothelial growth factor in ossification. *Int J Oral Sci* 2012; 4: 64–68.

39. Filipowska J, Tomaszewski KA, Niedźwiedzki Ł, et al. The role of vasculature in bone development, regeneration and proper systemic functioning. *Angiogenesis* 2017; 20: 291–302.

40. Diomede F, D'Aurora M, Gugliandolo A, et al. Biofunctionalized scaffold in bone tissue repair. *Int J Mol Sci* 2018; 19: 1022.

41. Carinci F, Palmieri A, Martinelli M, et al. Genetic portrait of osteoblast-like cells cultured on PerioGlas. *J Oral Implantol* 2007; 33: 327–333.